Journal of Nuclear Materials 400 (2010) 73–78

Contents lists available at ScienceDirect

Journal of Nuclear Materials

journal homepage: www.elsevier.com/locate/jnucmat

Effect of moisture on the self-healing of vitreous silica under irradiation

Glenn K. Lockwood, Stephen H. Garofalini *

Interfacial Molecular Science Laboratory, Department of Materials Science and Engineering, Rutgers University, Piscataway, NJ 08855, United States

ARTICLE INFO

Article history:
Received 22 December 2009
Accepted 10 February 2010

ABSTRACT

Although it is widely understood that water interacts extensively with vitreous silicates, atomistic simulations of the response of these materials to ballistic radiation, such as neutron or ion radiation, have excluded moisture. In this study, molecular dynamics simulations were used to simulate the collision cascades and defect formation that would result from such irradiation of silica in the presence of moisture. Using an interatomic potential that allows for the dissociation of water, it was found that the reaction between molecular water or pre-dissociated water (as OH^- and H^+) and the ruptured Si–O–Si bonds that result from the collision cascade inhibits a significant amount of the structural recovery that was previously observed in atomistic simulations of irradiation in perfectly dry silica. The presence of moisture not only resulted in a greater accumulation of non-bridging oxygen defects, but reduced the local density of the silica and altered the distribution of ring sizes. The results imply that an initial presence of moisture in the silica during irradiation could increase the propensity for further ingress of moisture via the low density pathways and increased defect concentration.

1. Introduction

Interactions between high-energy ballistic radiation and vitreous silica occur across a very diverse range of disciplines. For example, ions in solar wind can damage optics aboard spacecraft [1] and affect the structure and chemistry of lunar surface material [2,3], the optics for inertial confinement fusion are susceptible to damage from neutron irradiation [4,5], and the vitrified silicate waste forms being developed in many nations' nuclear waste management strategies must withstand extensive self-irradiation due to alpha decay [6–9]. Molecular dynamics (MD) simulations are ideally suited to simulating these interactions due to the length- and time-scales of collision cascades in silica, and they have been used to examine the atomic-scale phenomena that govern the response of silica to such radiation.

MD simulations of dry glasses have revealed picosecond-scale healing of local glass structure after a ballistic collision event such as would be caused by the recoil nucleus produced by alpha decay in a nuclear waste glass and it is believed that this rapid healing is at the center of vitreous silicates' resistance to radiation damage [5,10,11]. However, these simulations have generally been conducted in the absence of moisture for reasons of simplicity, yet water is known to interact extensively with the glassy network [12–22]. The interactions between ballistic radiation, the glassy network, and moisture govern the ultimate safety and viability of applications such as nuclear waste glasses and have been the subject of much experimentation over the last three decades [8,23–27], but it remains unclear what role moisture plays at the atomic level in these systems during irradiation.

In this study, MD simulations of repeated collision cascades in vitreous silica were performed both in the absence of water (as has been done in the past [5,10,11]) and in the presence of moisture (as may be expected in real waste glasses [28,29]). Because the interatomic potential used provides a completely atomistic description of all atomic interactions, these simulations allow for the dissociation of water and can capture the dynamic formation of hydrated silica sites such as silanol, as has been previously shown [22]. Thus, the effect of moisture on the self-healing of the amorphous silicate network can be assessed under conditions of ballistic irradiation.

2. Computational methods

The interatomic potential applied here has been used to accurately reproduce the properties and behavior of bulk water [30] and water interactions at the silica surface [22,31,32] in the past and is comprised of two- and three-body interactions. The two-body contribution, acting between atoms of type i and j, takes the general form

$$U_{ij}^{2\text{-}body}(r_{ij}) = U_{ij}^{q-q} + U_{ij}^{qd-qd} + U_{ij}^{q-qd} + U_{ij}^{qd-q} + U_{ij}^{rep} + U_{ij}^{disp} + U_{ij}^{12} \quad (1)$$

where each energy term is a function of the interatomic spacing r_{ij} and is given by

$$U_{ij}^{q-q}(r_{ij}) = \frac{q_i q_j}{r_{ij}} \cdot \mathrm{erfc}\left(\frac{r_{ij}}{\beta}\right) \quad (2)$$

* Corresponding author.
E-mail address: shg@rutgers.edu (S.H. Garofalini).

0022-3115/$ - see front matter © 2010 Elsevier B.V. All rights reserved.
doi:10.1016/j.jnucmat.2010.02.012

$$U_{ij}^{qd-qd}(r_{ij}) = \frac{q_i^d q_j^d}{r_{ij}} \mathrm{erf}\left(\frac{r_{ij}}{2\xi_{ij}}\right) \cdot \mathrm{erfc}\left(\frac{r_{ij}}{\beta}\right) \quad (3)$$

$$U_{ij}^{q-qd}(r_{ij}) = \frac{q_i q_j^d}{r_{ij}} \mathrm{erf}\left(\frac{r_{ij}}{\sqrt{2}\xi_{ij}}\right) \cdot \mathrm{erfc}\left(\frac{r_{ij}}{\beta}\right) \quad (4)$$

$$U_{ij}^{qd-q}(r_{ij}) = \frac{q_i^d q_j}{r_{ij}} \mathrm{erf}\left(\frac{r_{ij}}{\sqrt{2}\xi_{ij}}\right) \cdot \mathrm{erfc}\left(\frac{r_{ij}}{\beta}\right) \quad (5)$$

$$U_{ij}^{rep}(r_{ij}) = A_{ij}^{rep} \frac{2\xi_{ij}^r}{r_{ij}} \mathrm{erfc}\left(\frac{r_{ij}}{2\xi_{ij}^r}\right) \quad (6)$$

$$U_{ij}^{disp}(r_{ij}) = -\frac{C_{ij}^6}{r_{ij}^6} \quad (7)$$

$$U_{ij}^{12}(r_{ij}) = +\frac{B_{ij}^{12}}{r_{ij}^{12}} \quad (8)$$

The parameters used in this study are listed in Table I. ξ_{OH}^r is calculated as a function of temperature and pressure as described elsewhere [30], but the work in this study was all performed with a constant value of $\xi_{OH}^r = 0.02001$ nm which corresponds to $T = 298$ K and $P = 1$ atm. The calculated interactions between pairs are limited to atoms separated by a distance less than $R_c = 1$ nm, and as in past work, the long-range Coulomb interactions are determined by use of the Wolf summation method [33]. However, unlike the potential used previously, which is comprised of Eqs. (2)–(7), an additional U_{ij}^{12} term is used to offset the strong attraction caused by the U_{ij}^{disp} interaction at the very close interatomic spacings that may result from high-energy collision cascades. The point charges q and diffuse charges q^d assigned to each type of atom are listed in Table II.

The three-body portion of the interatomic potential is a function of the interatomic spacing of each triplet and the angle between them, and it is of the form

$$U_{jik}^{3-body}(r_{ij}, r_{jk}, \theta_{jik}) = \lambda_{jik} \exp\left(\frac{\gamma_{ij}}{r_{ij} - r_{ij}^0} + \frac{\gamma_{ik}}{r_{ik} - r_{ik}^0}\right)(\cos\theta_{jik} - \cos\theta_{jik}^0)^2 \quad (9)$$

The effect of this three-body contribution is to bias certain j–i–k atomic triplets towards certain angles to emulate the effects of bond directionality without preventing overcoordination, bond angle variations, or imposing any explicit rigidity as is often found in other common interatomic potentials for water. The parameters used are listed in Table III.

A vitreous silica sample was formed by melting a stoichiometric crystal of beta cristobalite containing 13,608 atoms by simulating a melt at 6000 K for 30,000 iterations with a 1 fs time step, then quenching it via intermediate temperatures to 298 K in a manner identical to past work [32]. The configuration that resulted from the melt-quench procedure was then simulated under conditions of constant temperature (298 K) and pressure (1 atm) for 40,000 steps. This system's final dimensions were 6.380 nm × 6.366 nm × 4.961 nm, and this configuration served as the basis for the dry system.

Table I
Two-body potential parameters.

i–j Pair	A_{ij}^{rep} (fJ)	ξ_{ij} (nm)	ξ_{ij}^r (nm)	B_{ij}^{12} (J nm^{12})	C_{ij}^6 (J nm^6)
O–H	0.2283	2.4	0.02001	0	0
O–O	0.0425	2.4	0.06100	4.0780×10^{-31}	4.2260×10^{-24}
H–H	0.0000	2.4	0.00000	0	0
Si–O	0.2670	2.4	0.03730	3.5000×10^{-31}	7.0000×10^{-24}
Si–Si	0.0700	2.4	0.06400	0	0
Si–H	0.5000	2.4	0.03500	5.6486×10^{-32}	3.8000×10^{-24}

Table II
Point and diffuse charges for each atom.

Ion	Si	O	H
Point charge q	+1.808e	−0.904e	+0.452e
Diffuse charge q^d	−0.452e	+0.226e	−0.113e

Table III
Three-body potential parameters.

j–i–k Triplet	λ_{jik} (fJ)	γ_{ij} (nm)	γ_{ik} (nm)	r_{ij}^0 (nm)	r_{ik}^0 (nm)	θ_{jik}^0
O–Si–O	0.0150	0.28	0.28	0.30	0.30	109.5
Si–O–Si	0.0010	0.20	0.20	0.28	0.28	109.5
H–O–H	0.0300	0.13	0.13	0.16	0.16	100.0
Si–O–H	0.0050	0.20	0.12	0.28	0.15	109.5

To generate the hydrated system, two approaches were taken: one approach using dissociated water, in which H^+ and OH^- ions were inserted near defect sites in the dry glass; the second approach involved incorporation of molecular water, which, because of the use of a dissociative water potential, could dissociate upon reaction with the silica. The use of ions in addition to the molecular water was done to minimize disruption to the silicate network before irradiation by encouraging the formation of SiOH without having to break additional bridging siloxane (Si–O–Si) bonds. For each non-bridging oxygen (Si–O^-) defect, a H^+ ion was inserted at a random position within 0.5 nm of the oxygen defect such that no other atoms were within 0.2 nm of the inserted H^+. Similarly, OH^- ions were inserted randomly within 0.5 nm of three-coordinated oxygen and three-coordinated silicon defects such that no atoms (aside from the hydrogen from the OH^-) was within 0.2 nm of the central oxygen of the OH^-. This resulting "wet" silica, containing 111 H^+ and 111 OH^- ions which correspond to a 2.38 mol% concentration of H_2O in silica, was allowed to relax at a constant temperature of 298 K and constant volume for 10,000 steps at a 0.1 fs time step. This was sufficiently long to eliminate any unphysically high-energy situations which may have arisen as a result of the randomized H^+/OH^- insertion yet brief enough to prevent extensive reaction and minimize deviation of the glassy network from the dry reference sample.

To ensure that this process of inserting dissociated water ions rather than molecular water did not produce any spurious results, another wet system was created by inserting 111 water molecules randomly throughout the glass such that no silica atoms were within 0.2 nm of the water molecule's oxygen atom. Unlike the other wet system, this glass with molecular water was not allowed to relax prior to the irradiation simulation. The results are very similar for the two different methods of incorporating water into the silica, so most of the results will be discussed in terms of the system involving incorporation of dissociated water (H^+ and OH^- ions). Due to the interesting features found in these systems containing 2.38 mol% water, a third hydrated silica was also generated by first inserting 111 H^+ and OH^- ions at defects sites (in a manner identical to that described above) and then inserting an additional 222 water molecules randomly. This corresponds to a concentration of 6.83 mol% water and represents what may be expected at near-surface region of a radiated glass in contact with water. This system was simulated under conditions of constant temperature (at 298 K) and volume for 10,000 iterations with a 0.1 fs time step prior to the irradiation simulation.

The overall method of simulating self-irradiation in the glass used here is similar to the method used by others [5,10]. To simulate the effects of a recoil nucleus, oxygen atoms at the center of the system were chosen at random and given an additional 1 keV of kinetic energy in a randomized direction. As a result of the very high atomic velocities immediately following the initiation of these recoil nuclei, the time step used between iterations was allowed to either decrease by a factor of 10 or increase by a factor of 5 such that no single atom moved more than 0.0012 nm between consecutive system configurations. Furthermore, to dissipate the heat inserted into the system as a result of these primary collision events, the velocities of atoms within 0.3 nm of the boundaries of the simulation box were rescaled to a temperature of 298 K every tenth iteration. Similarly, time steps were only allowed to be adjusted (if needed) every tenth step. Each system was simulated for approximately 35 ps, and each collision event was preceded by 2 ps of relaxation. Thus, at least 17 primary knock-on atoms (PKA) were initiated in all systems, each separated by 2 ps.

For the analysis, every 500th configuration was sampled throughout the course of the simulation, and due to the variable time step, this corresponded to a much higher sampling frequency (in s^{-1}) near primary collision events when nuclear velocities were very high.

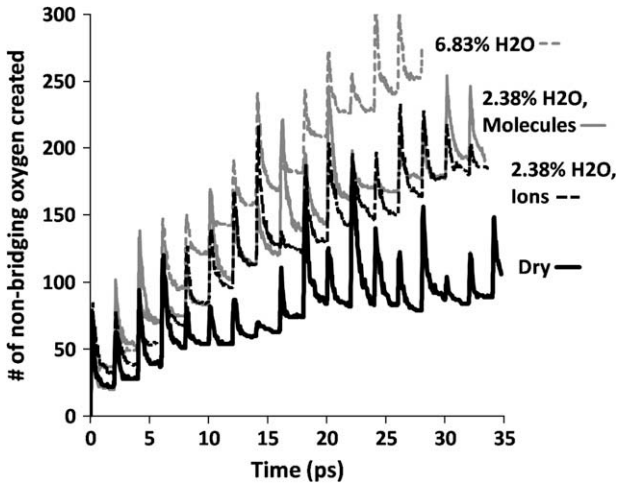

Fig. 1. Change in non-bridging oxygen defects over time; the time scale is defined such that the primary collision occurs at $t = 0$, and the change in defects is relative to this $t = 0$ value. The data considered are from silica without any water (labeled dry), silica with 2.38% water initially inserted as dissociated H^+ and OH^- (2.38% H_2O, ions), silica with 2.38% water initially in molecular form (2.38% H_2O, molecules), and silica with 6.83% inserted in both dissociated and molecular form (6.38% H_2O).

3. Results and discussion

3.1. Localized defect formation

The degree of network connectivity in silicate glasses is best gauged by the number of bridging oxygen atoms that join two neighboring silica tetrahedra. Thus, as a metric of the damage in the glassy network, the number of oxygen that did not have two silicon neighbors (hereafter referred to as non-bridging oxygen) were quantified over time. In the dry system, this was simply a count of how many oxygen atoms had only one silicon neighbor with a bonding distance less than 0.2 nm, where 0.2 nm is the minimum following the first-neighbor peak in the Si–O pair correlation function [15,34]. In the wet systems though, non-bridging oxygen in the simulation also were found to be bonded to one (in the case of silanol (Si–O–H)) or two (in the case of $Si–OH_2^+$) hydrogen ions at a distance less than 0.12 nm, consistent with both experimental data [35] and other computations [17,22]. Thus, Si–O, Si–O–H, and $Si–OH_2$ species all contribute to the non-bridging count in the wet systems.

Fig. 1 depicts the change in counts for non-bridging oxygens in wet and dry systems. The systems display the characteristic spike in defect concentration coincident with the primary collision event, followed by rapid, picosecond-scale structural recovery as reported by others (cf. Fig. 1 in [5]). However, the extent of network repolymerization following the first decay event is less pronounced in the wet systems than it is in the dry system and this divergence becomes increasingly pronounced with successive hits. Although the magnitude of the individual defect peaks may vary due to the random nature of the PKA trajectories and the glassy network, the response of the glass to radiation was far more strongly affected by the presence of any type of moisture than it was by the starting form of the moisture, whether it was dissociated water or molecular water. Thus, unless otherwise noted, the following discussion regards observations in the system created with dissociated water rather than molecular water, and at a concentration of 2.38 mol%. The data from the 6.83 mol% data will be discussed separately below.

The number of silanol groups and free hydroxyls measured over the course of the irradiation is shown in Fig. 2, and it illustrates the reaction of the free hydroxyl groups as the glass is damaged by collision cascades. Each data point in this figure (except the first and last) represents the concentration immediately before a new collision, thereby reflecting the concentration after the maximum possible recovery time between consecutive hits. Of the original 111 OH^- added to the glass, 46 remained as free OH^- after the short relaxation that preceded the irradiation and this is shown by the first data point. Those remaining free OH^- reacted rapidly with the undercoordinated silicon (SiO_3) that formed as the collision cascade disrupted the network connectivity. This is evidenced by the nearly 1:1 correlation between SiOH formed and OH^- destroyed during the 10 ps following the first collision in Fig. 2.

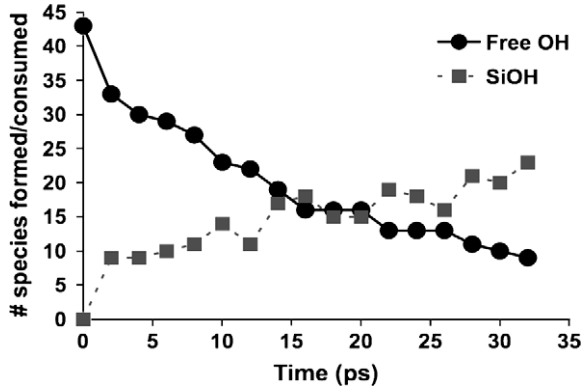

Fig. 2. Number of SiOH and OH^- throughout irradiation simulation. SiOH data represent changes relative to the starting concentration. Free OH is the total number of unbound OH^- in the system. Each data point represents the count in the system configuration sampled immediately before collision events, which is representative of the maximum relaxation time allowed during irradiation, and the time scale is defined such that the first primary collision occurs at $t = 0$.

The result of this were SiOH groups which prevented the recombination of non-bridging oxygen and undercoordinated silicon and therefore prevented healing of the glassy network; the formation of a bridge from these hydrated groups would require a condensation reaction. While several water molecules were observed to form during the simulation, all but two dissociated again, resulting in no net restoration of bridges from hydrated defects. Of the two H_2O molecules that did not re-react though, both were the

product of OH^- groups that had never reacted with Si. Thus, while the H^+ with which these two ions reacted could have been released as the result of a bridge reforming, no instances of two neighboring silanol groups reacting to form a Si–O–Si bridge and H_2O molecule were observed.

These reactions between the hydrous species and the silica network were accelerated by the high temperatures of the system; although the edges of the simulation box were maintained at 298 K, the center of the system experienced a brief thermal spike with a mean temperature in excess of 1100 K immediately following each collision event. This temperature rapidly cooled to 400–600 K between successive collision events, allowing the rapid formation of SiOH at sites broken in the defect track.

3.2. Ring size evolution

To assess the extent of this effect moisture has on the self-healing of the longer-range network connectivity, the ring size distribution for each system was also calculated over the course of the simulations. Five- and six-membered rings (rings consisting of five or six silicon tetrahedra) constituted the greatest fraction of rings before irradiation, consistent with bulk glass structure. In both

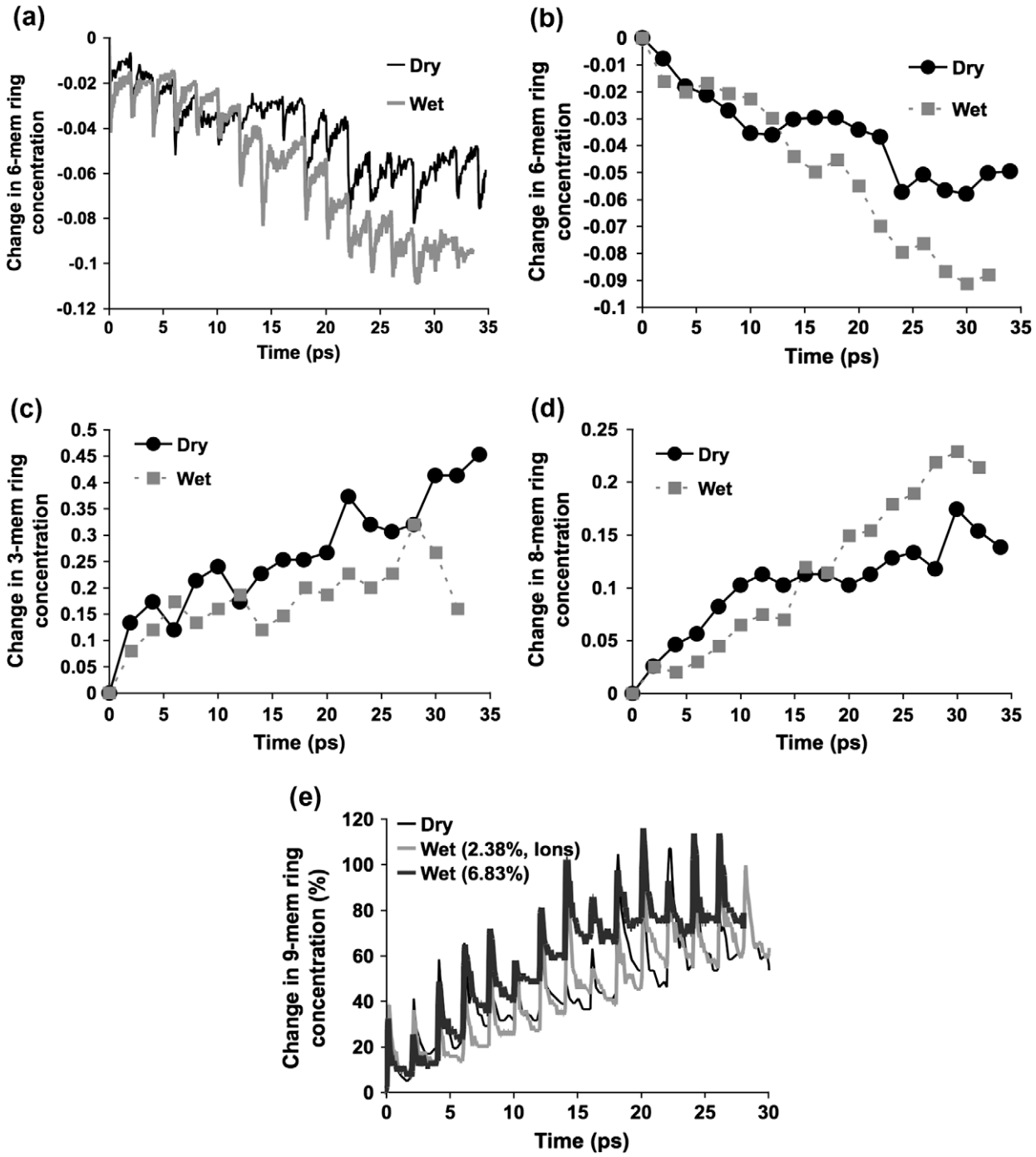

Fig. 3. Change in ring concentration over time for six-membered rings sampled at (a) every 500 iterations and (b) immediately before each primary collision, representative of the maximum relaxation time allowed during irradiation. Also shown are (c) three-membered rings and (d) eight-membered rings sampled immediately preceding each primary collision and (e) rings with nine or more silicon tetrahedra sampled every 500 iterations.

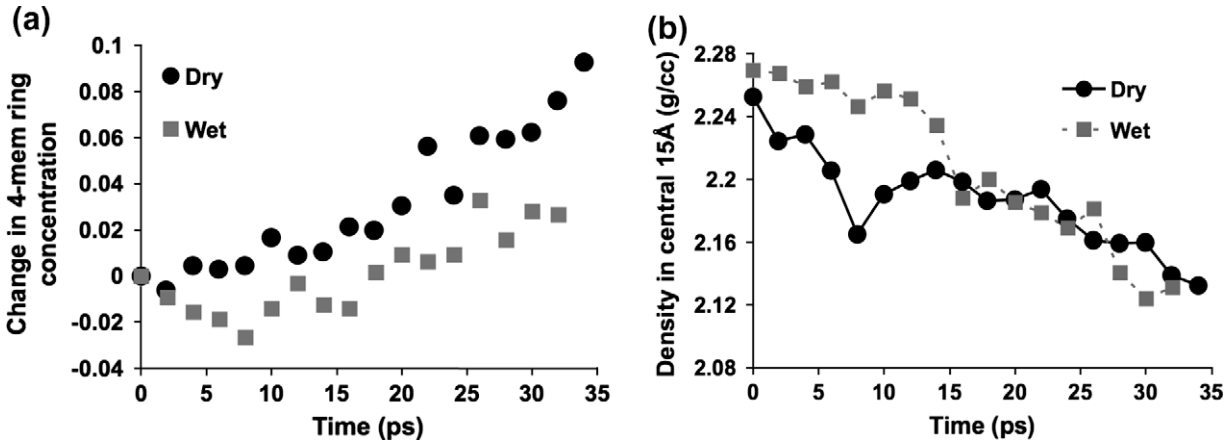

Fig. 4. (a) Change in concentration of four-membered rings and (b) density of the central 1.5 nm of the system as a function of time during irradiation taken at the configuration preceding each primary collision.

wet and dry glass systems, each primary collision event caused the rapid rupture of five- and six-membered rings, followed by limited recovery, as shown for the six-membered rings in Fig. 3a. This behavior is similar in fashion to the formation and healing of non-bridging defects shown in Fig. 1, with the wet systems showing less recovery than the dry system at longer time. Fig. 3b shows the fraction change in six-membered rings at configurations immediately preceding each primary collision event (thus allowing for relaxation from the previous collision event); the five-membered ring concentration reflected a similar decrease over the course of the irradiation. This cumulative damage in the form of five- and six-membered ring rupture is consistent with other simulations of dry silica [5,36].

Much of the structural recovery that followed each primary collision event resulted in the net increase in the number of three-membered rings (Fig. 3c) and rings with eight and nine or more silicon tetrahedra (Fig. 3d and e). The formation of the small three-membered rings is very consistent with the formation of such rings at dry silica surfaces; the smaller concentration of these rings in the wet system is consistent with their reaction with moisture upon hydration, forming silanols [15,21,37–42], lowering their concentration. As shown in Fig. 3c, the concentration of three-membered rings increased by between 16% and 32% towards the end of the simulation in the wet system and by between 32% and 45% in the dry system, suggesting that water has the effect of inhibiting the formation of strained three-membered rings during self-healing. Furthermore, by assuming that the rates of increase in these rings are constant after the initial period of rapid increase when $t < 10$ ps, fitting a straight line to the data for $t > 10$ ps in Fig. 3 gives an indication of how quickly these rings are forming. Doing this reveals that the three-membered ring concentration increases at a rate of 0.901%/ps in the dry system and about half of that, 0.454%/ps, in the wet system under the simulated radiative flux.

Four-membered rings showed a net increase during the course of the irradiation, but this increase in concentration only began after about 8 ps under irradiation or four primary collision events. Furthermore, as shown in Fig. 4a, the number of these rings decreased during the beginning of the simulation in the wet system, then began increasing after this ~8 ps "incubation" period. This delay may be related to the limited availability of moisture near the four-membered ring as irradiation proceeds. However, there may also be an effect of local density. Examining the density of a spherical volume of $r = 1.5$ nm, whose center coincides with the center of the simulation box, indicates that the increase in four-membered ring formation occurs in the dry system as density initially decreases with irradiation, as shown in Fig. 4b, suggesting that the formation of these rings occurs after a critical amount of excess volume is made available for localized structural rearrangement. While complicated by the presence of moisture in the wet system, there is also an increase in the concentration of four-membered rings as the glass density decreases. At irradiation levels where the densities of both systems reach the same value and begin to decrease at similar rates, the rate of four-membered ring formation in both systems also appears to increase at a similar rate.

Studies on the polymerization of silica have shown that four-membered rings are the smallest rings that can form with no significant strain in the bridging oxygen bond between silica tetrahedra [15,43,44]. Thus, whereas three-membered rings are necessarily strained and are typically formed as a mechanism for surface relaxation, four-membered rings can form at any region where there is enough volume for rearrangement and the temperature is sufficiently high to permit the necessary kinetics. While five- and six-membered rings can also form under similar conditions, the fact that they are larger results in a larger probability of rupture during the course of a collision cascade, and these rings undergo a net decrease as damage accumulates.

The formation of the large membered rings is indicative of nanoscale 'void' formation that plays a significant role in the rupture of silica glass under stress [45–48]. A clear divergence is seen in the number of eight-membered rings, with the wet system showing a larger fraction increase, but the nine and larger membered ring plot shows similar behavior for the wet system with 2.38% water and dry systems, with only a hint of divergence at the longer times. The enhanced formation of the larger (eight and nine or more) rings in the wet system implies a weakening of the silica during irradiation to a greater extent than that for the dry system.

Furthermore, the formation of these low-density regions near the glass surface also allows water to penetrate deeper into the subsurface [22,49]. To gain insight into the effect of such an increase in subsurface water concentration, silica with 6.83 mol% H_2O was subjected to irradiation, and this system showed a significantly greater degree of defect formation, as shown in Figs. 1 and 3e. In the latter, the increased moisture caused an increase in the formation of the largest rings, although the concentration appears to maximize near 80% increase, which may be the limit of formation of such large rings. Thus, the damage due to irradiation compounds more quickly in the presence of increasing moisture, and this in turn increases the formation of large voids and lowers density. Based on these results, it becomes easy to envision this accelerated damage due to water as a self-propagating process where

damage opens volume, allowing external water to diffuse into the glassy network more easily and further accelerate the accumulation of damage.

4. Conclusions

The simulations of dry silica glass exposed to irradiation are consistent with previous simulations that had shown considerable self-healing of broken bonds, offering a mechanism for the resistance of silica to ballistic radiation. However, the current simulations show that the presence of moisture in the silica network has the significant effect of inhibiting the extent to which broken bonds reform, thus limiting structural recovery. The degree of non-bridging oxygen formation and retention in the presence of water is enhanced when moisture reacts with Si–O–Si bonds broken by irradiation, allowing for a more open network structure that could affect further ingress of moisture into the glass. Retention of larger rings in the wet silica implies a weakening of the glass, similar to that seen in previous studies of the fracture of silica glass. Because moisture can be expected in current waste glass compositions, understanding the atomistic behavior of radiation-induced damage in silicates requires the consideration of the reactions between water and the glassy network and its effect on structural recovery.

Acknowledgement

GKL acknowledges support from the Advanced Fuel Cycle Initative University Fellowship sponsored by the DOE Office of Nuclear Energy.

References

[1] G. Naletto, A. Boscolo, J. Wyss, A. Quaranta, Appl. Optics 42 (2003) 3970–3980.
[2] G. Strazzulla, J.R. Brucato, G. Cimino, G. Leto, F. Spinella, Adv. Space. Res. 15 (1995) (10)13–(10)17.
[3] E.J. Zeller, L.B. Ronca, P.W. Levy, J. Geophys. Res. 71 (1966) 4855–4860.
[4] A. Kubota, M.-J. Caturla, S.A. Payne, T. Diaz de la Rubia, J.F. Latkowski, J. Nucl. Mater. 307–311 (2002) 891–894.
[5] A. Kubota, M.-J. Caturla, J. Stolken, B. Sadigh, S. Reyes, T. Diaz de la Rubia, J.F. Latkowski, Nucl. Instr. Meth. Phys. Res. B 202 (2003) 88–92.
[6] W.G. Burns, A.E. Hughes, J.A.C. Marples, R.S. Nelson, A.M. Stoneham, Nature 295 (1982) 130–132.
[7] J.M. Delaye, D. Ghaleb, Nucl. Instr. Meth. Phys. Res. B 135 (1998) 201–206.
[8] S. Peuget, J.-N. Cachia, C. Jegou, X. Deschanels, D. Roudil, V. Broudic, J.M. Delaye, J.-M. Bart, J. Nucl. Mater. 354 (2006) 1–13.
[9] D.J. Wronkiewicz, Effects of Radionuclide Decay on Waste Glass Behavior – A Critical Review, Report ANL-93/45, Argonne National Laboratory, 1993.
[10] J.M. Delaye, D. Ghaleb, Phys. Rev. B 61 (2000) 14481–14494.
[11] J.M. Delaye, D. Ghaleb, Phys. Rev. B 71 (2005) 224204-1–224204-10.
[12] R.K. Iler, The Chemistry of Silica, John Wiley and Sons, New York, 1979.
[13] V. Bolis, B. Fubini, L. Marchese, G. Martra, D. Costa, J. Chem. Soc. Faraday Trans. 87 (1991) 497–505.
[14] I.-S. Chuang, G.E. Maciel, J. Am. Chem. Soc. 118 (1996) 401–406.
[15] B.P. Feuston, S.H. Garofalini, J. Appl. Phys. 68 (1990) 4830–4836.
[16] B.A. Morrow, I.A. Cody, J. Phys. Chem. 80 (1976) 1998–2004.
[17] J.R. Rustad, E. Wasserman, A.R. Felmy, C. Wilke, J. Colloid Interface Sci. 198 (1998) 119–129.
[18] D.W. Sindorf, E. Maciel, J. Am. Chem. Soc. 105 (1983) 1487–1493.
[19] D.A. Sverjensky, N. Sahai, Geochem. Cosmochem. Acta 62 (1998) 3703–3716.
[20] L.T. Zhuravlev, Langmuir 3 (1987) 316–318.
[21] E.B. Webb, S.H. Garofalini, J. Non-Cryst. Solid 226 (1998) 47–57.
[22] T.S. Mahadevan, S.H. Garofalini, J. Phys. Chem. C 112 (2008) 1507–1515; J. Phys. Chem. C 113 (2009) 11177.
[23] A. Abbas, Y. Serruys, D. Ghaleb, J.M. Delaye, B. Boizot, B. Reynard, G. Calas, Nucl. Instr. Meth. Phys. Res. B 166–167 (2000) 445–450.
[24] J.K. Bates, L.J. Jardine, M.J. Steindler, The Hydration Process of Nuclear-Waste Glass: An Interim Report ANL-82-11, Argonne National Laboratory, 1982.
[25] J.C. Dran, M. Maurette, J.C. Petit, Science 209 (1980) 1518–1520.
[26] W. Primak, Nucl. Technol. 60 (1983) 199–205.
[27] J. Wald, F. Roberts, Comm. Am. Ceram. Soc. (1984) 69–70.
[28] H. Li, M. Tomozawa, J. Non-Cryst. Solid 195 (1996) 188–198.
[29] S.K. Sundaram, S. Thevuthasan, D.E. McCready, Mater. Res. Soc. Symp. Proc. 556 (1999) 353–358.
[30] T.S. Mahadevan, S.H. Garofalini, J. Phys. Chem. B 111 (2007) 8919–8927.
[31] S.H. Garofalini, T.S. Mahadevan, S. Xu, G.W. Scherer, ChemPhysChem 9 (2008) 1997–2001.
[32] G.K. Lockwood, S.H. Garofalini, J. Chem. Phys. 131 (2009) 074703.
[33] D. Wolf, P. Keblinski, S.R. Phillpot, J. Eggebrecht, J. Chem. Phys. 110 (1999) 8254–8282.
[34] H. Morikawa, S. Miwa, M. Miyake, F. Marumo, T. Sata, J. Am. Ceram. Soc. 65 (1982) 78–81.
[35] Y. Duval, J.A. Mielczarski, O.S. Pokrovsky, E. Mielczarske, J.J. Ehrhardt, J. Phys. Chem. B 106 (2002) 2937–2945.
[36] F. Mota, M.-J. Caturla, J.M. Perlado, J. Molla, A. Ibarra, J. Nucl. Mater. 386–388 (2009) 75–78.
[37] C.J. Brinker, R.K. Brow, D.R. Tallant, R.J. Kirkpatrick, J. Non-Cryst. Solid 120 (1990) 26–33.
[38] C.J. Brinker, R.J. Kirkpatrick, D.R. Tallant, B.C. Bunker, B. Montez, J. Non-Cryst. Solid 99 (1988) 418–428.
[39] F.L. Galeener, A.J. Leadbetter, M.W. Stringfellow, Phys. Rev. B 27 (1983) 1052–1078.
[40] F. Galeener, J. Mikkelsen, Phys. Rev. B 23 (1981) 5527–5530.
[41] S.H. Garofalini, J. Non-Cryst. Solid 120 (1990) 1–12.
[42] J.D. Kubicki, D. Sykes, Phys. Chem. Miner. 19 (1993) 381–391.
[43] S.H. Garofalini, G. Martin, J. Phys. Chem. 98 (1994) 1311–1316.
[44] L.L. Hench, J.K. West, Chem. Rev. 90 (1990) 33–72.
[45] E. Bouchaud, J. Phys. Cond. Matter 9 (1997) 4319–4344.
[46] F. Célarié, S. Prades, D. Bonamy, Phy. Rev. Lett. 90 (2003) 075504-1-4.
[47] K. Muralidharan, J.H. Simmons, P.A. Deymier, K. Runge, J. Non-Cryst. Solid 351 (2005) 1532–1542.
[48] T.P. Swiler, J.H. Simmons, A.C. Wright, J. Non-Cryst. Solid 182 (1995) 68–77.
[49] A.E. Kohler, S.H. Garofalini, Langmuir 10 (1994) 4664–4669.